Computed Tomography Imaging Analysis of the MPFL Femoral Footprint Morphology and the Saddle Sulcus

Evaluation of 1094 Knees

Jiebo Chen,* MD, Yijia Xiong,† BS, Kang Han,* MBBS, Caiqi Xu,* MD, Jiangyu Cai,* MD, Chenliang Wu,* MD, Zipeng Ye,* MD, Jinzhong Zhao,*‡ MD, and Guoming Xie,*‡ MD

Investigation performed at Shanghai Jiao Tong University Affiliated Sixth People's Hospital, Shanghai, China

Background: The medial patellofemoral ligament (MPFL) has been reported to be anatomically attached from an osseous saddle region (saddle sulcus) between neighboring landmarks on the femur, including the adductor tubercle (AT), medial epicondyle (ME), and medial gastrocnemius tubercle (MGT). However, the position and prevalence of the saddle sulcus remain unknown.

Purpose: To study the femoral footprint of MPFL and the prevalence of the saddle sulcus with computed tomography (CT) imaging; quantify the position of the saddle sulcus; and determine the relevant factors of the identified position and measuring distances.

Study Design: Cross-sectional study; Level of evidence, 3.

Methods: A total of 1094 knees in 753 patients were studied. Knees were organized into an anterior cruciate ligament reconstruction (ACLR) group (controls) and a recurrent patellar dislocation (RPD) group. Using 3-dimensionally reconstructed CT images, the authors determined the prevalence of the saddle sulcus and its position relative to the AT, the ME, the Schöttle point (1.3 mm anterior to the distal posterior cortex and 2.5 mm distal to the posterior origin of the medial femoral condyle), and the Fujino point (approximately 10 mm distal to the AT). Analysis of covariance was used to adjust for age, sex, side, and body mass index on the measurements.

Results: There were 555 knees in the control group and 539 knees in the RPD group. The MPFL femoral footprint presented as an oblique, oblong, osseous region (saddle sulcus) in 75.7% of knees (75.0%, ACLR group vs 76.4%, RPD group; $P < .001$). The saddle sulcus was located a mean of 12.2 mm (95% CI, 12.0-12.4 mm) from a line connecting the apex of the AT to the ME (AT-ME) and a mean of 7.6 mm (95% CI, 7.5-7.8 mm) posteriorly perpendicular to that line. The location as a proportion of the AT-ME distance was 63.1% (95% CI, 62.6%-63.7%) in the *X* direction and 39.8% (95% CI, 39.1%-40.5%) in the *Y* direction. The Schöttle and Fujino points lay anterior and proximal to the saddle sulcus more than 5 mm away from the center of the saddle sulcus. Women had a higher prevalence of saddle sulcus (odds ratio [OR], 1.33 [95% CI, 1.00-1.75]; $P = .046$) compared with men.

Conclusion: The saddle sulcus was identified in 75.7% of knees from the medial femoral aspect, with its center located consistently between the AT and ME.

Keywords: medial patellofemoral ligament; patellar dislocation; femur; footprint, saddle sulcus

Patellar dislocation constitutes 3.3% of all knee injuries,[29] affecting 23 per 100,000 people in the United States annually over 21 years.[40] Medial patellofemoral ligament (MPFL) injury occurs in >85% of primary patellar dislocations.[23,51] Recurrent patellar dislocation (RPD) occurs after nonoperative treatment in one-third to one-half of patients with acute patellar dislocations.[43,60] Thus, MPFL reconstruction is becoming more common. However, 47% of major postoperative complications have resulted from technical problems during MPFL reconstruction, and 68% of technical problems are a result of nonanatomic femoral positioning.[33]

Radiographic reference points have often been used to determine the femoral tunnel position.[4,17,37,41,47,55] However, the accuracy of this method has been debated,[9,22,38,39,60] and the difficulty in obtaining true-lateral radiographs during

The Orthopaedic Journal of Sports Medicine, 10(2), 23259671211073608
DOI: 10.1177/23259671211073608

surgery adds to the confusion. Recently, direct assessment of the femoral anatomy has been proposed for MPFL femoral tunnel placement.[58,60] Bicos et al[7] were the first to characterize a saddle region where the MPFL originated from the femoral aspect. Baldwin[3] and Ziegler et al[60] also described the MPFL as being consistently and anatomically attached from the osseous saddle region between neighboring landmarks, including the adductor tubercle (AT), medial epicondyle (ME), and medial gastrocnemius tubercle (MGT).

In previous studies[11,58] we confirmed such findings; termed the bony region as the *saddle sulcus*, which could be identified on 3-dimensionally (3D) reconstructed computed tomography (CT) images; and determined that intraoperative palpation was feasible through a small incision. However, there are gaps that need to be systematically addressed. First, it is potentially time-consuming and difficult for novice surgeons to palpate the saddle sulcus. Second, for patients who do not have an obvious bony sulcus, it is necessary to create a reference position from those who do. Finally, there is little research detailing the MPFL femoral footprint in the RPD population.

This study is a follow-up CT imaging analysis to our previous in vitro study.[11] We aimed to (1) determine the CT imaging morphology of the MPFL footprint on the femur and the general prevalence of the saddle sulcus in patients with and without RPD; (2) quantify the position of the saddle sulcus in each group and determine the individualized positioning during MPFL reconstruction; and (3) determine the relevant factors of the identified position and measuring distances. We hypothesized that the saddle sulcus is present in 75% of knees and is consistently located surrounding the AT and ME, with a nonsignificant difference between patients with and without RPD.

METHODS

Study Design

Data recorded from 2015 to 2020 in our institution were used for cross-sectional analysis. The study protocol was approved by the institutional ethics committee of the Shanghai Sixth People's Hospital, and we followed the STROBE (Strengthening the Reporting of Observational Studies in Epidemiology) reporting guidelines for cross-sectional studies.[54] Informed consent was waived because of the retrospective nature of the study.

Study Population

Control Group. The control group consisted of patients clinically diagnosed with anterior cruciate ligament (ACL) injury on the basis of radiographic findings and clinical and intraoperative arthroscopic examinations. Patients were included who underwent CT within 3 days after ACL reconstruction (ACLR), as routinely performed in our clinical practice for reexamining tunnel positioning.

RPD Group. The study group included patients who were diagnosed with RPD with trochlear dysplasia by radiologic findings and clinical examinations. This group was divided into 4 subgroups according to the Dejour classification of femoral trochlea on both axial CT scans and digitally reconstructed images[13,14,27,50]: type A (shallow trochlear sulcus/crossing sign), type B (flat or convex trochlea/suprathrochlear bump or spur), type C (hypoplastic medial facet with lateral convexity/double contour), and type D (cliff-shaped trochlea/vertical join or cliff pattern).

Exclusion Criteria

Patients in the ACLR group were excluded from the study if they had patellofemoral instability, femoral trochlear dysplasia, or patella alta (calculated by Caton-Deschamps index[10]). Regardless of grouping, patients with the following conditions were excluded: (1) severe patellofemoral or tibiofemoral osteopathy or osteoarthritis, (2) skeletal immaturity, (3) multiple ligament injuries, (4) damaged femoral ME (ie, previous MPFL surgery), and (5) insufficient CT image quality (ie, images with severe artifacts).

CT Imaging

CT scans on all patients were performed through a multidetector CT scanner (Lightspeed VCT 64; GE), with a 120-kV tube voltage, 350-mA tube current, 0.625-mm reconstructive slice and interval thickness, and 1.0-second rotation time. The imaging measurements of both groups were conducted by an experienced surgeon (J.C.) using 3D CT–reconstructed standard mediolateral knee images.[34] Direct distances on the reconstructed femurs were calculated using Digimizer image analysis software (MedCalc Software Ltd).

Two senior orthopaedic surgeons and 1 musculoskeletal radiologist (J.Z., G.X, and Y.X.) reviewed all the 3D images and axial CT scans to determine the osseous landmarks, including the apexes of the AT, ME, and MGT. The AT was

‡Address correspondence to Jinzhong Zhao, MD, Department of Sports Medicine, Shanghai Jiao Tong University Affiliated Sixth People's Hospital, 600 Yishan Road, Shanghai, 200233, China (email: jzzhao@sjtu.edu.cn or Guoming Xie, MD, Department of Sports Medicine, Shanghai Jiao Tong University Affiliated Sixth People's Hospital, 600 Yishan Road, Shanghai, 200233, China (email: xieguoming2006@163.com).

*Department of Sports Medicine, Shanghai Jiao Tong University Affiliated Sixth People's Hospital, Shanghai, China.

†Department of Radiology, Shanghai Jiao Tong University Affiliated Sixth People's Hospital, Shanghai, China.

J. Chen, Y.X., and K.H. contributed equally to this study.

Final revision submitted October 8, 2021; accepted November 8, 2021.

One or more of the authors has declared the following potential conflict of interest or source of funding: Support was received from the National Key Research and Development Program of China (grants 2018YFC1106200 and 2018YFC1106202), the National Natural Science Foundation of China (grant 81871753), and the Exploratory Research Program of Shanghai Jiao Tong University Affiliated Sixth People's Hospital (grant YNTS202001). AOSSM checks author disclosures against the Open Payments Database (OPD). AOSSM has not conducted an independent investigation on the OPD and disclaims any liability or responsibility relating thereto.

Ethical approval for this study was obtained from Shanghai Sixth People's Hospital (approval No. 2020-KY-031(K)).

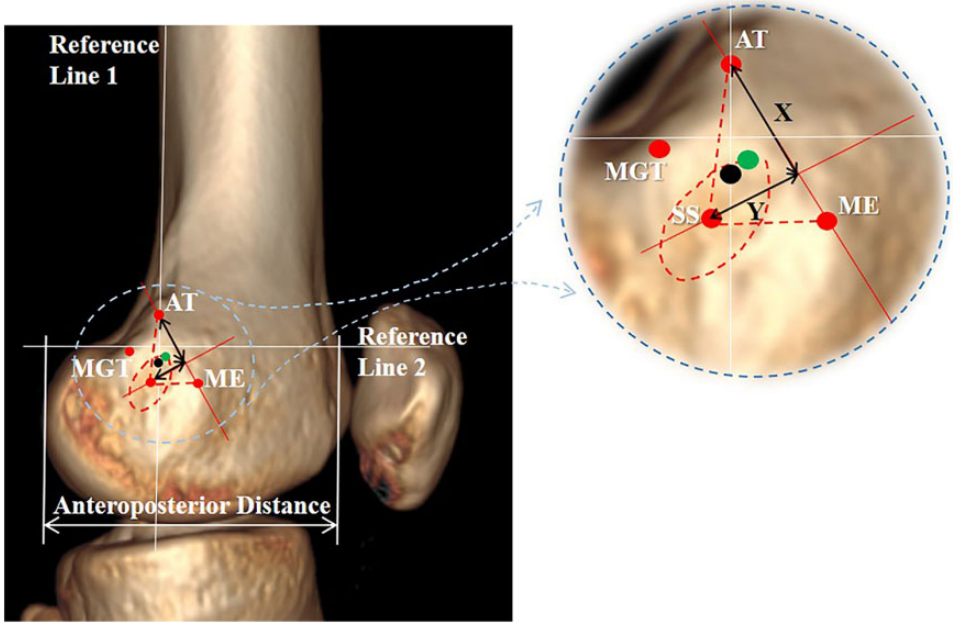

Figure 1. A 3-dimensional computed tomography–reconstructed left knee from the standard mediolateral view, marked with the osseous landmarks (red dots). Reference line 1 extends distally along the posterior femoral cortex, and reference line 2 intersects the contact point of the apex of the medial epicondyle (ME) and the posterior cortex. The anteroposterior distance of the medial femoral condyle was measured according to Stephen et al.[47] The inset shows the Schöttle point (black dot) and Fujino point (green dot). Distance *Y* was defined from the center of the saddle sulcus (SS) to the line connecting the apex of the adductor tubercle (AT) and ME, and distance *X* was the perpendicular distance from distance *Y* to the AT. MGT, apex of the medial gastrocnemius tubercle.

consistent in the femoral medial and posterior aspects,[17] with a prominence located between the femoral medial condyle and the shaft. Considering the variability in the ME (eg, flat or shallow groove shape),[17] the axial image of the CT scan at which the ME was the most prominent was used to determine the apex. Because of its relatively large tendon insertion and variability of existence,[60] the MGT was identified to confirm the location of the saddle sulcus. No measurements were performed based on this tubercle so as to avoid any underlying measurement error.

The saddle sulcus has been anatomically[3,58,60] and radiographically[11] identified as an osseous depression or region where the MPFL is consistently attached. Considering previous descriptions of the MPFL femoral footprint,[1,21,24,48,52] we thus determined the saddle sulcus on the reconstructed femur as (1) being located within the boundaries of the AT, ME, and MGT; (2) lying posterior to the border connecting the apexes of the AT and ME; and (3) a broad, oblong, and oblique saddle-like sulcus. The 3D-reconstructed model was rotated to ultimately determine the presence of the saddle sulcus.

Distance Measurements

The center of the saddle sulcus was defined using distances *X* and *Y*, as shown in Figure 1. Based on this location, we calculated the distance from the saddle sulcus center to the AT (SS-AT), the ME (SS-ME), and 2 previously reported radiographic reference points: the Schöttle point[41] (1.3 mm anterior to the distal posterior cortex and 2.5 mm distal to the posterior origin of the medial femoral condyle; SS-Schöttle) and the Fujino point[17] (approximately 10 mm distal to the AT; SS-Fujino). In addition, we calculated the proportion of distance *X* and distance *Y* to the AT-ME distance (*X*/AT-ME% and *Y*/AT-ME%, respectively) for standardization and heat mapping analysis.

The anteroposterior width of the ME was calculated according to Stephen et al[47] to standardize the measurements in different population sizes (Figure 1). The normalized measurements (M_n) were calculated as follows:

$$M_n = M_o \times (\overline{AP}/AP)$$

where M_o is the original measurement, $\overline{AP}$ is the average of all measured anteroposterior distances of the ME, and AP is the anteroposterior distance of the ME.

Study Outcomes

The primary study outcomes were the MPFL femoral footprint morphology and the prevalence and position of the saddle sulcus. A heat map was created to provide a visual representation of the identified sulcus centers as distributed over the femoral medial condyle using *X*/AT-ME% and *Y*/AT-ME%. The secondary outcomes were the other measurements (SS-AT, SS-ME, AT-ME, *X*, *Y*, SS-Schöttle, and SS-Fujino).

TABLE 1
Comparison of Baseline Characteristics in the ACLR and RPD Groups, 2015-2020[a]

	Overall (n = 1094[b])	ACLR Group (n = 555)	RPD Group (n = 539)[c]	MD (95% CI)	*P*
Patient age, y	28.3 ± 8.8	30.8 ± 8.5	24.4 ± 8.0	6.4 (5.2-7.6)	**<.001**
Female sex	322/753 (42.8)	114/453 (25.2)	208/300 (69.3)	—	**<.001**
Body mass index, kg/m^2	24.5 ± 3.8	24.8 ± 3.5	24.0 ± 4.2	0.8 (0.3-1.4)	**.004**
Right side affected	553 (50.5)	282 (50.8)	271 (50.3)	—	.860
AP width of medial condyle, mm	60.6 ± 4.8[d]	62.9 ± 4.3	58.3 ± 4.2	4.6 (4.0-5.2)	**<.001**

[a]Values are reported as mean ± SD or n (%). Bolded *P* values indicate a statistically significant difference between the study groups ($P < .05$). ACLR, anterior cruciate ligament reconstruction; AP, anteroposterior; MD, mean difference; RPD, recurrent patellar dislocation.
[b]Number of knees.
[c]The Dejour classification of femoral trochlea was as follows: 19 type A (3.5%), 31 type B (5.8%), 321 type C (59.6%), and 168 type D (31.2%).
[d]There was no significant difference in AP width between right and left knees (60.7 ± 4.8 vs 60.6 ± 4.8 mm, respectively; $P = .886$).

Statistical Analysis

A descriptive analysis of the study population was completed for continuous (mean) and discrete (percentage) variables. The normality of continuous data was evaluated using the Shapiro-Wilk test. Independent-sample *t* tests (continuous variables) and chi-square tests (discrete variables) were used to compare baseline characteristics between the 2 groups. The Mann-Whitney *U* test was used for nonnormal data. A binary logistic regression model was used to determine the associations of the prevalence of the saddle sulcus with group differentiation and demographic factors. Analysis of covariance (ANCOVA) models were used to adjust for covariates such as age, sex, side, and body mass index (BMI) on the imaging measurements. Bonferroni adjustments were also performed for multiple comparisons. We performed a subgroup analysis of the RPD group by femoral trochlear morphology (Dejour classification); linear regression analysis was used to evaluate the difference in the saddle sulcus measurements between subgroups, with the ACLR group set as a dummy variable. All statistical analyses were performed using SPSS (24.0; IBM Corp), with statistical significance set at $P < .05$ and with 2-sided tests.

Intraclass correlation coefficients (ICCs) were calculated to evaluate intraobserver and interobserver reliabilities of the measurements. To determine the intraobserver reliability, 100 patients in each group were randomly chosen for the primary observer (J.C.) to reperform the measurements 2 weeks later in a separate sitting position. To determine the interobserver reliability, a second blinded observer (K.H.) completed the measurements on the same 100 patients independently. An ICC $\geq$0.75 was considered good, 0.50 to 0.74 moderate, and <0.50 poor.[32,42]

RESULTS

Baseline Characteristics

We analyzed 1094 knees from 753 patients; there were 555 knees (50.7%) in the ACLR group and 539 knees (49.3%) in the RPD group. The overall mean (± SD) age was 28.3 ± 8.8 years, and 322 patients (42.8%) were women (Table 1). The overall anteroposterior ME width was 60.6 ± 4.8 mm. The intra- and interobserver ICCs of the measurements were both good (0.86 [95% CI, 0.81-0.90] and 0.81 [95% CI, 0.74-0.86], respectively).

Overall Quantified Anatomic Features

The MPFL femoral footprint presented as 4 predominant shapes on the 3D CT–reconstructed images as follows: (1) saddle sulcus; (2) dimple; (3) "fake" groove; and (4) "fusion" mound (Figure 2).

The saddle sulcus, when present, was an oblique, oblong, osseous region sitting between the AT, ME, and MGT, which were identified on the reconstructed knee images (Figure 2, A-C). With the diverse range of femoral attachment width of MPFL as 11.5 ± 4.3 mm,[21] this fan-like structure occasionally originated at a dimple-like osseous region, with a smaller width. It could be considered a subtype of the saddle sulcus. Additionally, "fake" grooves, as formed by the ME,[17] were excluded according to the aforementioned definition of the saddle sulcus. Because the tubercles on the femoral medial aspect might merge together as a mound, no specific osseous depression could be identified under this condition (Figure 2).

Prevalence and Position of the Saddle Sulcus

The overall prevalence of the saddle sulcus was 75.7% (75.0% in the ACLR group and 76.4% in the RPD group; $P < .001$). The saddle sulcus was located 12.2 mm (95% CI, 12.0-12.4 mm) from the apex of the AT according to distance *X* and 7.6 mm (95% CI, 7.5-7.8 mm) perpendicular to distance *X* according to distance *Y*. The location as a proportion of the AT-ME distance was 63.1% (95% CI, 62.6%-63.7%) for *X*/AT-ME% and 39.8% (95% CI, 39.1%-40.5%) for *Y*/AT-ME% (Table 2).

Significant unadjusted differences in the imaging measurements were observed between the ACLR and RPD groups on all variables except for *X*/AT-ME% (Table 2). The differences in the measurements for SS-ME, distance *Y*, and SS-Fujino became nonsignificant after adjustment by the testing models (Figure 3 and Table S1 in the Supplemental Material).

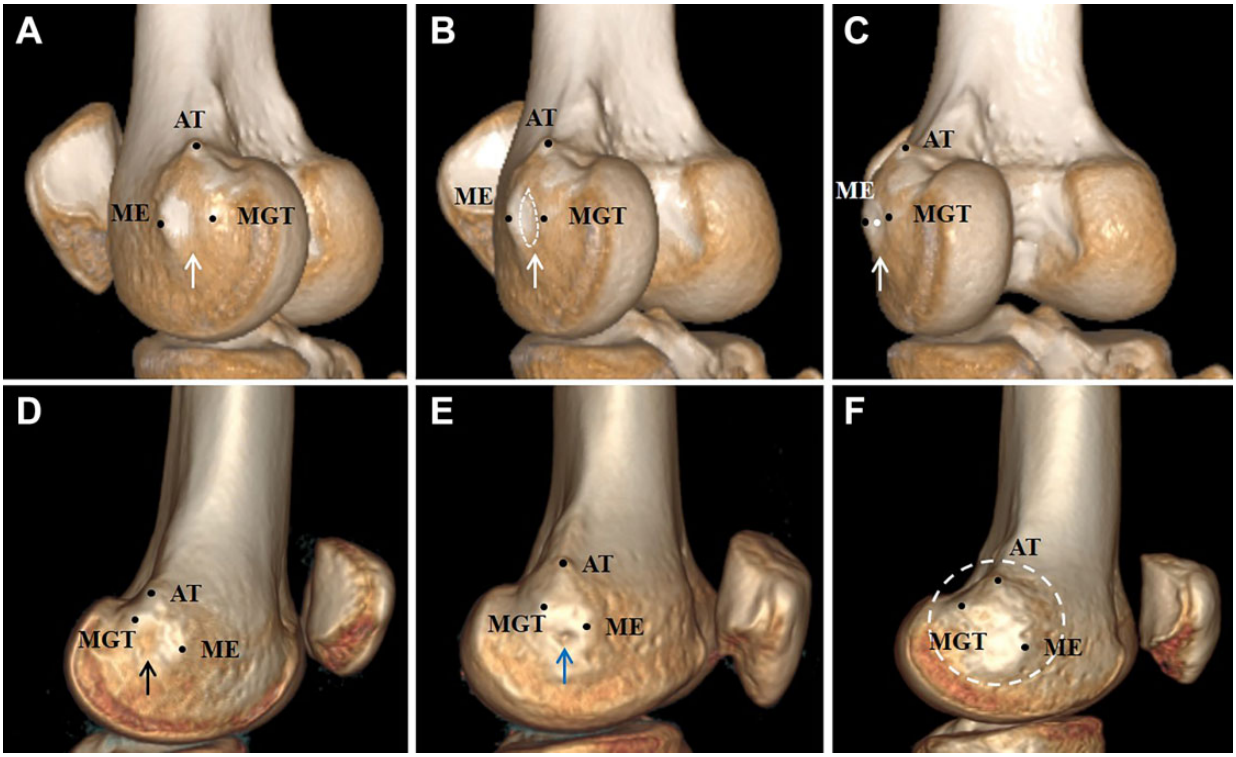

Figure 2. Description of the medial patellofemoral ligament femoral insertion on 3-dimensionally reconstructed knees. (A-C) The saddle sulcus from oblique posterior femoral views (white arrows); (B) the saddle region and (C) center of the region were marked. (D) Dimple (black arrow). (E) "Fake" groove (blue arrow). (F) "Fusion" mound (dashed white circle). AT, apex of the adductor tubercle; ME, apex of the medial epicondyle; MGT, apex of the medial gastrocnemius tubercle.

TABLE 2
Overall and Unadjusted Group Differences for Saddle Sulcus Prevalence and CT Measurements[a]

	Overall (n = 828)[b]	ACLR Group (n = 416)	RPD Group (n = 412)	MD (95% CI)	*P*
Prevalence of saddle sulcus, %	75.7	75.0	76.4	—	**<.001**
Distance, mm					
SS-AT	14.5 (14.3 to 14.7)	15.0 (14.7 to 15.3)	14.0 (13.7 to 14.3)	1.0 (0.6 to 1.5)	**<.001**
SS-ME	10.5 (10.3 to 10.7)	11.1 (10.9 to 11.4)	9.9 (9.7 to 10.1)	1.3 (0.9 to 1.6)	**<.001**
AT-ME	19.2 (19.0 to 19.5)	19.8 (19.5 to 20.2)	18.7 (18.3 to 19.0)	1.1 (0.7 to 1.6)	**<.001**
X	12.2 (12.0 to 12.4)	12.4 (12.2 to 12.7)	11.9 (11.6 to 12.2)	0.5 (0.1 to 0.9)	**.007**
Y	7.6 (7.5 to 7.8)	8.2 (7.9 to 8.4)	7.1 (6.9 to 7.3)	1.1 (0.7 to 1.4)	**<.001**
SS-Schöttle	8.3 (8.1 to 8.5)	7.9 (7.6 to 8.2)	8.8 (8.5 to 9.1)	–0.9 (–1.3 to –0.5)	**<.001**
SS-Fujino	5.5 (5.3 to 5.7)	6.0 (5.7 to 6.3)	5.0 (4.7 to 5.2)	1.0 (0.7 to 1.4)	**<.001**
X/AT-ME%	63.1 (62.6 to 63.7)	62.6 (61.8 to 63.4)	63.6 (63.0 to 64.3)	–1.0 (–2.1 to 0.1)	.064
Y/AT-ME%	39.8 (39.1 to 40.5)	41.4 (40.4 to 42.4)	38.2 (37.3 to 39.2)	3.2 (1.8 to 4.6)	**<.001**

[a]See the Methods section for definitions of the distances. Values are reported as mean (95% CI) unless otherwise indicated. Bolded *P* values indicate statistically significant difference between the study groups ($P < .05$). ACLR, anterior cruciate ligament reconstruction; AT, apex of the abductor tubercle; CT, computed tomography; MD, mean difference; ME, apex of the medial epicondyle; RPD, recurrent patellar dislocation; SS, center of the saddle sulcus.

[b]Number of knees with identified saddle sulcus on the CT scan.

All identified saddle sulci were depicted in the femoral medial aspect (Figure 4). The mean SS-Schöttle and SS-Fujino distances both exceeded 5 mm, and the reference points mainly lay anterior and proximal to the saddle sulcus.

Women carried a 33% higher prevalence of saddle sulcus (OR, 1.33 [95% CI, 1.00-1.75], $P = .046$) compared with men. Increased BMI, male sex, left side, and patellar instability were related to usually greater measuring distances in the ANCOVA model for adjustment. Decreased BMI ($P = .040$)

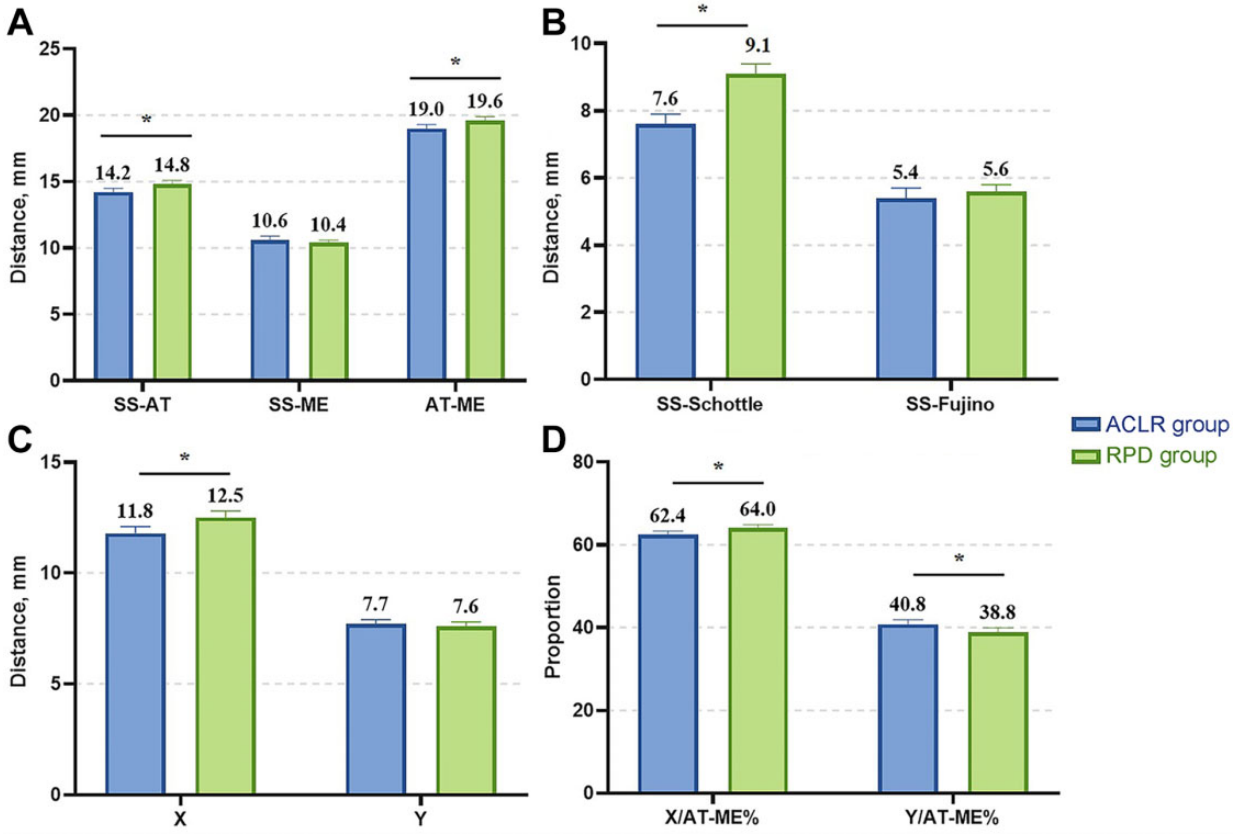

Figure 3. Adjusted differences between the anterior cruciate ligament reconstruction (ACLR) and recurrent patellar dislocation (RPD) groups in the measurements for (A) SS-AT, SS-ME, and AT-ME distances; (B) SS-Schöttle and SS-Fujino; (C) distance *X* and distance *Y*; and (D) *X*/AT-ME% and *Y*/AT-ME%. Error bars indicate 95% CIs. AT, apex of the adductor tubercle; ME, apex of the medial epicondyle; SS, center of the saddle sulcus. See the Methods section for definitions of the distances. *Statistically significant difference ($P < .05$).

and patellar instability ($P = .023$) predicted a lower *Y*/AT-ME% (Table S2 in the Supplemental Material).

Subgroup Analysis for the RPD Group

No statistical differences were detected within the RPD subgroups either before or after adjustment for confounding factors, except for the adjusted SS-Schöttle distance (Dejour type A vs type D: 6.9 mm [95% CI, 5.6-8.3] vs 9.1 mm [95% CI, 8.7-9.6], $P = .018$) (Table S3 in the Supplemental Material). The calculations for *X*/AT-ME% ($R^2 = 0.021$, $P = .001$), distance *X* ($R^2 = 0.214$, $P < .001$), SS-AT ($R^2 = 0.257$, $P < .001$), AT-ME ($R^2 = 0.263$, $P < .001$), and SS-Schöttle ($R^2 = 0.071$, $P < .001$) were significantly increased in patients with Dejour type C compared with those of the ACLR group.

DISCUSSION

The main findings of this study were that (1) MPFL femoral footprint morphology varies and presents as an oblique, oblong, osseous region (saddle sulcus) identified in 75.7% knees (75.0% [ACLR group], 76.4% [RPD group]) in 3D-reconstructed models; and (2) the position of the saddle sulcus center was approximately 12 mm (approximately 60% of the AT-ME distance) from the apex of the AT per distance *X* and 7 to 8 mm (approximately 40% of the AT-ME distance) perpendicular to distance *X* per distance *Y* (60%-40% rule, namely the simple method to determine the saddle sulcus center using proportions) (Figure 3), which was consistent with slight differences in each group. The study findings suggest that it is feasible to palpate the saddle sulcus during surgery, as it could be identified in 75.7% knees, and the 60%-40% rule could be used as a potential guidance by identifying AT and ME in patients with no obvious saddle region.

Concerns have been raised that patients at risk of RPD have anatomically different knees, particularly for the femoral trochlear shapes.[9,20,39,50] Thus, previous laboratory studies[9,38] using healthy cadaveric knees would not be fully relied on in routine clinical practice. Patellofemoral kinematics, contact area and pressure, and stability were further reported to be significantly affected by trochlear dysplasia in a simulated in vitro test.[53] Therefore, in

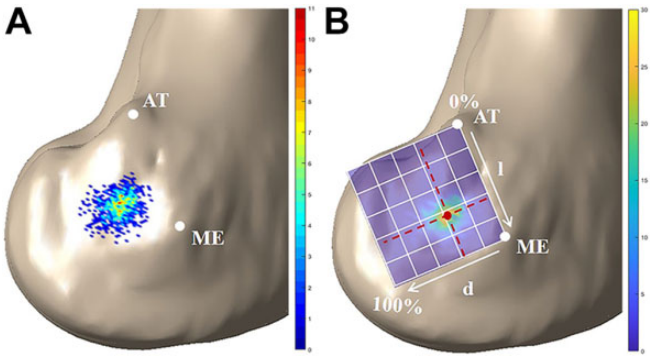

Figure 4. Heat map illustrating the distribution of all identified centers of the saddle sulcus or dimple over the medial aspect of the medial femoral epicondyle relative to the apex of the adductor tubercle (AT) and apex of the medial epicondyle (ME) from a true mediolateral view of the left reconstructed knee in extension. (A) The darkest blue area on the femur shows the least distributed attachment area, while yellow areas highlight areas with a high degree of distribution. (B) A grid was applied to the medial femoral condyle, with line *l* connecting the AT and ME and line *d* perpendicular to line *l*; lines *l* and *d* were identical in length. The dashed red perpendicular lines represent the average position of the saddle sulcus (red dot).

cadaveric studies with a relatively small sample size, it would be necessary to include an adequate population with RPD to assess the femoral medial anatomic features.

The synthesis location of the saddle sulcus demonstrated a consistent region, located at a triangular space,[1,21] and varied between neighboring bony landmarks.[2,25,30,35] We quantified the saddle sulcus position with normalized dimensions (60%-40% rule) of the femoral surface geometry to minimize the positioning error from variance. Additionally, we found that the location of the saddle sulcus in the RPD group was statistically significantly anteroproximal to the control group, while the absolute differences were clinically small at 1 to 2 mm. In clinical practice, for patients without an identified saddle sulcus (24.3%), the 60%-40% rule could be used as a potential guidance by identifying AT and ME. However, the tunnel placement still requires further validation in other work before it can be considered clinically actionable.

The Schöttle point and Fujino point lay anterior and proximal (>5 mm outranging) relative to the saddle sulcus, a nonneglectable malposition causing potentially dramatic patellofemoral pressure increase and alteration of graft isometry.[15,45-47] The consistent radiographic reference points did not take into consideration the variation of the bony architecture, and their use has been argued against for ensuring anatomic positioning.[22,38,39,60] Moreover, the length change pattern of MPFL has been investigated mostly based on Schöttle point[6,18,44] or Fujino point[31,57] as the anatomic femoral insertion. Our findings thus provide a novel insight into such length change pattern studies with the saddle sulcus as the MPFL femoral footprint. And potentially a more anatomic length change pattern and the relative tolerable error of varying femoral positionings could be found and further studied.

Most of the imaging measurements were significantly greater in male patients, left knees, and patients with increased BMI. The knee size was significantly different between sexes,[16,56] and men had a generally larger femoral shape.[16] Femoral geometry increased with BMI,[5,59] although the increment was not commensurate.[5] Regarding the side factor, numerous studies[12,19,36] found no contour differences in the femur between sides. However, ACL femoral insertion differed significantly between right and left knees measured by Dargel et al,[12] suggesting potential surface morphology differences between sides with similar contours. After adjusting for confounding factors, most distance measurements in the RPD group, especially with Dejour type C femoral trochlea, were significantly increased compared with those in the control group. The results indicated that patients with medial trochlear dysplasia could be at risk not only of patellofemoral instability[26] but also of surface morphology alterations, including the osseous landmarks' relative positions on the medial aspect.

The main strengths of the study are its (1) sample size, which to our knowledge is the largest to date in a systematic imaging analysis study of MPFL femoral origin in RPD and ACLR population; (2) confounding factors adjustment and analysis, which have never been presented before in such a series study; and (3) systematic comparison with radiographic reference points.

The weaknesses of the study are as follows. First, patients with ACLR rather than a healthy population with no knee injuries were included as the control group. Although this population was previously reported as comparable with patellofemoral instability,[8,9] and ACLR did not damage the femoral medial condyle, the underlying differences might prevent the generalization of our results. Second, the determination of the geometric centers of the osseous landmarks could be influenced by the image quality and understanding of the saddle sulcus. However, all the images were obtained with 0.625-mm reconstructive thickness, and the intraobserver and interobserver reliabilities of the described methods were found to be good (ICC, >0.8),[28,42] suggesting that the 60%-40% rule is feasible to use in routine clinical practice. Third, only patients with both RPD and femoral trochlear dysplasia were included for analysis. Patients with RPD without femoral trochlear dysplasia, acute patellar dislocation, and patellofemoral pain should be investigated in further studies. Fourth, the study evaluated saddle sulcus only by CT. The relation between the saddle sulcus and the MPFL femoral insertion, and the functionality of the ligament inserted at this point require further evaluations. Moreover, the evolving understanding of the medial patellar complex shows that the medial quadriceps tendon–femoral ligament, medial patellotibial ligament, and medial patellomeniscal ligament might also help to medially stabilize the patella.[49] However, only MPFL reconstruction was included for consideration to treat patellar instability in our study.

CONCLUSION

The study findings indicated that there are variations in the morphology of the MPFL femoral footprint. An oblique, oblong, osseous region (saddle sulcus) was identified in 75.7% of knees from the medial femoral aspect, with its center located between the AT and ME and following the 60%-40% rule for individualized positioning. The Schöttle point and Fujino point may differ in location for tunnel positioning guidance. This study provides further information in determining the femoral tunnel position during MPFL anatomic reconstruction and in studies on length change patterns.

ACKNOWLEDGMENT

The authors thank Cong Wang, BSc, and Tsung-Yuan Tsai, PhD, from the Department of Orthopaedic Surgery and Orthopaedic Biomechanical Laboratory, School of Biomedical Engineering, Shanghai Jiao Tong University, for their help in making the heat map.

Supplemental material for this article is available at http://journals.sagepub.com/doi/suppl/10.1177/23259671211003521.

REFERENCES

1. Aframian A, Smith TO, Tennent TD, Cobb JP, Hing CB. Origin and insertion of the medial patellofemoral ligament: a systematic review of anatomy. *Knee Surg Sports Traumatol Arthrosc*. 2017;25(12):3755-3772.
2. Amis AA, Firer P, Mountney J, Senavongse W, Thomas NP. Anatomy and biomechanics of the medial patellofemoral ligament. *Knee*. 2003;10(3):215-220.
3. Baldwin JL. The anatomy of the medial patellofemoral ligament. *Am J Sports Med*. 2009;37(12):2355-2361.
4. Barnett AJ, Howells NR, Burston BJ, et al. Radiographic landmarks for tunnel placement in reconstruction of the medial patellofemoral ligament. *Knee Surg Sports Traumatol Arthrosc*. 2012;20(12):2380-2384.
5. Beck TJ, Petit MA, Wu G, et al. Does obesity really make the femur stronger? BMD, geometry, and fracture incidence in the Women's Health Initiative-Observational Study. *J Bone Miner Res*. 2009;24(8):1369-1379.
6. Belkin NS, Meyers KN, Redler LH, et al. Medial patellofemoral ligament isometry in the setting of patella alta. *Arthroscopy*. 2020;36(12):3031-3036.
7. Bicos J, Fulkerson JP, Amis A. Current concepts review: the medial patellofemoral ligament. *Am J Sports Med*. 2007;35(3):484-492.
8. Biedert RM, Albrecht S. The patellotrochlear index: a new index for assessing patellar height. *Knee Surg Sports Traumatol Arthrosc*. 2006;14(8):707-712.
9. Campos T, Soogumbur A, McNamara IR, Donell ST. The trochlear isometric point is different in patients with recurrent patellar instability compared to controls: a radiographical study. *Knee Surg Sports Traumatol Arthrosc*. 2018;26(9):2797-2803.
10. Caton J.Method of measuring the height of the patella. Article in French. *Acta Orthop Belg*. 1989;55(3):385-386.
11. Chen J, Han K, Jiang J, et al. Radiographic reference points do not ensure anatomic femoral fixation sites in medial patellofemoral ligament reconstruction: a quantified anatomic localization method based on the saddle sulcus. *Am J Sports Med*. 2021;49(2):435-441.
12. Dargel J, Feiser J, Gotter M, Pennig D, Koebke J. Side differences in the anatomy of human knee joints. *Knee Surg Sports Traumatol Arthrosc*. 2009;17(11):1368-1376.
13. Dejour D, Le Coultre B. Osteotomies in patella-femoral instabilities. *Sports Med Arthrosc Rev*. 2007;15(1):39-46.
14. Dejour D, Saggin P. The sulcus deepening trochleoplasty—the Lyon's procedure. *Int Orthop*. 2010;34(2):311-316.
15. Elias JJ, Cosgarea AJ. Technical errors during medial patellofemoral ligament reconstruction could overload medial patellofemoral cartilage: a computational analysis. *Am J Sports Med*. 2006;34(9):1478-1485.
16. Fan L, Xu T, Li X, Zan P, Li G. Morphologic features of the distal femur and tibia plateau in southeastern Chinese population: a cross-sectional study. *Medicine (Baltimore)*. 2017;96(46):e8524.
17. Fujino K, Tajima G, Yan J, et al. Morphology of the femoral insertion site of the medial patellofemoral ligament. *Knee Surg Sports Traumatol Arthrosc*. 2015;23(4):998-1003.
18. Geier A, Tischer T, Bader R. Simulation of varying femoral attachment sites of medial patellofemoral ligament using a musculoskeletal multibody model. *Curr Dir Biomed Eng*. 2015;1(1):547-551.
19. Harrington KI, Wescott DJ. Size and shape differences in the distal femur and proximal tibia between normal weight and obese American Whites. *J Forensic Sci*. 2015;60(suppl 1):S32-S38.
20. Hopper GP, Leach WJ, Rooney BP, Walker CR, Blyth MJ. Does degree of trochlear dysplasia and position of femoral tunnel influence outcome after medial patellofemoral ligament reconstruction? *Am J Sports Med*. 2014;42(3):716-722.
21. Huber C, Zhang Q, Taylor WR, et al. Properties and function of the medial patellofemoral ligament: a systematic review. *Am J Sports Med*. 2020;48(3):754-766.
22. Izadpanah K, Meine H, Kubosch J, et al. Fluoroscopic guided tunnel placement during medial patellofemoral ligament reconstruction is not accurate in patients with severe trochlear dysplasia. *Knee Surg Sports Traumatol Arthrosc*. 2020;28(3):759-766.
23. Kang HJ, Wang F, Chen BC, Zhang YZ, Ma L. Non-surgical treatment for acute patellar dislocation with special emphasis on the MPFL injury patterns. *Knee Surg Sports Traumatol Arthrosc*. 2013;21(2):325-331.
24. Kruckeberg BM, Chahla J, Moatshe G, et al. Quantitative and qualitative analysis of the medial patellar ligaments: an anatomic and radiographic study. *Am J Sports Med*. 2018;46(1):153-162.
25. LaPrade RF, Engebretsen AH, Ly TV, et al. The anatomy of the medial part of the knee. *J Bone Joint Surg Am*. 2007;89(9):2000-2010.
26. Levy BJ, Tanaka MJ, Fulkerson JP. Current concepts regarding patellofemoral trochlear dysplasia. *Am J Sports Med*. 2021;49(6):1642-1650.
27. Lippacher S, Dejour D, Elsharkawi M, et al. Observer agreement on the Dejour trochlear dysplasia classification: a comparison of true lateral radiographs and axial magnetic resonance images. *Am J Sports Med*. 2012;40(4):837-843.
28. Mahomed N, Gandhi R, Daltroy L, Katz JN. The self-administered patient satisfaction scale for primary hip and knee arthroplasty. *Arthritis*. 2011;2011:591253.
29. Majewski M, Susanne H, Klaus S. Epidemiology of athletic knee injuries: a 10-year study. *Knee*. 2006;13(3):184-188.
30. Nomura E, Inoue M, Osada N. Anatomical analysis of the medial patellofemoral ligament of the knee, especially the femoral attachment. *Knee Surg Sports Traumatol Arthrosc*. 2005;13(7):510-515.
31. Oka S, Matsushita T, Kubo S, et al. Simulation of the optimal femoral insertion site in medial patellofemoral ligament reconstruction. *Knee Surg Sports Traumatol Arthrosc*. 2014;22(10):2364-2371.
32. Parada SA, Eichinger JK, Dumont GD, et al. Accuracy and reliability of a simple calculation for measuring glenoid bone loss on 3-dimensional computed tomography scans. *Arthroscopy*. 2018;34(1):84-92.

33. Parikh SN, Nathan ST, Wall EJ, Eismann EA. Complications of medial patellofemoral ligament reconstruction in young patients. *Am J Sports Med*. 2013;41(5):1030-1038.
34. Pfeiffer TR, Burnham JM, Hughes JD, et al. An increased lateral femoral condyle ratio is a risk factor for anterior cruciate ligament injury. *J Bone Joint Surg Am*. 2018;100(10):857-864.
35. Philippot R, Chouteau J, Wegrzyn J, et al. Medial patellofemoral ligament anatomy: implications for its surgical reconstruction. *Knee Surg Sports Traumatol Arthrosc*. 2009;17(5):475-479.
36. Pinsornsak P, Chaiwuttisak A, Boontanapibul K. Risk factors and outcomes in asymmetrical femoral component size for posterior referencing bilateral total knee arthroplasty: a matched pair analysis. *BMC Musculoskelet Disord*. 2018;19(1):294.
37. Redfern J, Kamath G, Burks R. Anatomical confirmation of the use of radiographic landmarks in medial patellofemoral ligament reconstruction. *Am J Sports Med*. 2010;38(2):293-297.
38. Sanchis-Alfonso V, Ramirez-Fuentes C, Montesinos-Berry E, Aparisi-Rodriguez F, Marti-Bonmati L. Does radiographic location ensure precise anatomic location of the femoral fixation site in medial patellofemoral ligament surgery? *Knee Surg Sports Traumatol Arthrosc*. 2016;24(9):2838-2844.
39. Sanchis-Alfonso V, Ramirez-Fuentes C, Montesinos-Berry E, Elia I, Marti-Bonmati L. Radiographic location does not ensure a precise anatomic location of the femoral fixation site in medial patellofemoral ligament reconstruction. *Orthop J Sports Med*. 2017;5(11):232596 7117739252.
40. Sanders TL, Pareek A, Hewett TE, et al. Incidence of first-time lateral patellar dislocation: a 21-year population-based study. *Sports Health*. 2018;10(2):146-151.
41. Schöttle PB, Schmeling A, Rosenstiel N, Weiler A. Radiographic landmarks for femoral tunnel placement in medial patellofemoral ligament reconstruction. *Am J Sports Med*. 2007;35(5):801-804.
42. Shrout PE, Fleiss JL. Intraclass correlations: uses in assessing rater reliability. *Psychol Bull*. 1979;86(2):420-428.
43. Sillanpää PJ, Peltola E, Mattila VM, et al. Femoral avulsion of the medial patellofemoral ligament after primary traumatic patellar dislocation predicts subsequent instability in men: a mean 7-year nonoperative follow-up study. *Am J Sports Med*. 2009;37(8):1513-1521.
44. Song SY, Pang CH, Kim CH, et al. Length change behavior of virtual medial patellofemoral ligament fibers during in vivo knee flexion. *Am J Sports Med*. 2015;43(5):1165-1171.
45. Stephen JM, Kaider D, Lumpaopong P, Deehan DJ, Amis AA. The effect of femoral tunnel position and graft tension on patellar contact mechanics and kinematics after medial patellofemoral ligament reconstruction. *Am J Sports Med*. 2014;42(2):364-372.
46. Stephen JM, Kittl C, Williams A, et al. Effect of medial patellofemoral ligament reconstruction method on patellofemoral contact pressures and kinematics. *Am J Sports Med*. 2016;44(5):1186-1194.
47. Stephen JM, Lumpaopong P, Deehan DJ, Kader D, Amis AA. The medial patellofemoral ligament: location of femoral attachment and length change patterns resulting from anatomic and nonanatomic attachments. *Am J Sports Med*. 2012;40(8):1871-1879.
48. Tanaka MJ. Femoral origin anatomy of the MPFC: implications for reconstruction. *Arthroscopy*. 2020;36(12):3010-3015.
49. Tanaka MJ, Chahla J, Farr J II, et al. Recognition of evolving medial patellofemoral anatomy provides insight for reconstruction. *Knee Surg Sports Traumatol Arthrosc*. 2019;27(8):2537-2550.
50. Tecklenburg K, Dejour D, Hoser C, Fink C. Bony and cartilaginous anatomy of the patellofemoral joint. *Knee Surg Sports Traumatol Arthrosc*. 2006;14(3):235-240.
51. Tompkins MA, Rohr SR, Agel J, Arendt EA. Anatomic patellar instability risk factors in primary lateral patellar dislocations do not predict injury patterns: an MRI-based study. *Knee Surg Sports Traumatol Arthrosc*. 2018;26(3):677-684.
52. Trinh TQ, Ferrel JR, Bentley JC, Steensen RN. The anatomy of the medial patellofemoral ligament. *Orthopedics*. 2017;40(4):e583-e588.
53. Van Haver A, De Roo K, De Beule M, et al. The effect of trochlear dysplasia on patellofemoral biomechanics: a cadaveric study with simulated trochlear deformities. *Am J Sports Med*. 2015;43(6): 1354-1361.
54. von Elm E, Altman DG, Egger M, et al. The Strengthening the Reporting of Observational Studies in Epidemiology (STROBE) statement: guidelines for reporting observational studies. *Int J Surg*. 2014;12(12): 1495-1499.
55. Wijdicks CA, Griffith CJ, LaPrade RF, et al. Radiographic identification of the primary medial knee structures. *J Bone Joint Surg Am*. 2009; 91(3):521-529.
56. Wise BL, Liu F, Kritikos L, et al. The association of distal femur and proximal tibia shape with sex: the Osteoarthritis Initiative. *Semin Arthritis Rheum*. 2016;46(1):20-26.
57. Yoo YS, Chang HG, Seo YJ, et al. Changes in the length of the medial patellofemoral ligament: an in vivo analysis using 3-dimensional computed tomography. *Am J Sports Med*. 2012; 40(9):2142-2148.
58. Zhang X, Xie G, Zhang C, et al. Comparation and evaluation of the accuracy of the sulcus localization method to establish the medial patellofemoral ligament femoral tunnel: a cadaveric and clinical study. *BMC Musculoskelet Disord*. 2019;20(1):53.
59. Zhao LJ, Jiang H, Papasian CJ, et al. Correlation of obesity and osteoporosis: effect of fat mass on the determination of osteoporosis. *J Bone Miner Res*. 2008;23(1):17-29.
60. Ziegler CG, Fulkerson JP, Edgar C. Radiographic reference points are inaccurate with and without a true lateral radiograph: the importance of anatomy in medial patellofemoral ligament reconstruction. *Am J Sports Med*. 2016;44(1):133-142.